 doi:10.20944/preprints202210.0068.v1

Article

Optimized Power Pads for Charging ElectricVehicles Based on a New Rectangular Spiral Shape Design

Benalia Nadir [1]*, Kouider Laroussi [1], Benlaloui Idriss [2] , Kouzou Abdellah [1,3,4], Abed-Djebar Bensalah [2] , Ralph Kennel[4], Mohamed Abdelrahem[4,5]*

[1] Department of electrical engineering, Laboratory of Applied Automation and Industrial Diagnostics (LAADI), Faculty of Science and Technology, Ziane Achour University, 17000, Djelfa, Algeria. nadir.Benalia@univ-djelfa.dz (N.B), kouider.laroussi@univ-djelfa.dz (L.K), a.kouzou@univ-djelfa.dz (K.A)
[2] Department of electrical engineering, Laboratory LSPIE, University of Batna 2, Algeria i.benlaloui@univ-batna2.dz (I.B), a.bensalah@univ-batna2.dz (B.A)
[3] Electrical and Electronics Engineering Department, Nisantasi University, Istanbul 34398, Turkey;
[4] Technical University of Munich (TUM), 80333 Munich, Germany; ralph.kennel@tum.de (R.K)
[5] Faculty of Engineering, Assiut University, Assiut 71516, Egypt; Mohamed.abdelrahem@aun.edu.eg (M.A.)

* Correspondence: i.benlaloui@univ-batna2.dz and Mohamed.abdelrahem@tum.de

Abstract: Optimizing the magnetic coupling of two coils of a dynamic wireless charging power supply for electric vehicles (EVs) is a challenging and crucial task. This article examines three situations of the magnetic coupling between two identical rectangular spiral coils with the same number of turns as a function of both the horizontal (X axis) and vertical (Z axis) alignment. In the first one, the analysis of the magnetic coupling between two copper air coils is presented. However, the obtained coupling coefficient was very low with a high leakage flux which affected the performance of the charging system. In the second case, a straightforward shielding method that involves inserting a magnetic material of the ferrite type is proposed to circumvent the aforementioned problems. Unfortunately, the obtained results show that simple shielding is still only a partial and insufficient solution. In the third situation, an aluminum sheet was consequently placed on the top of the ferrite to provide an adequate shielding structure. Additionally, a 3D analysis of the proper and mutual induction parameters separating the two coils as well as a magnetic field or induction distribution is also performed using the ANSYS Maxwell software. The results highlight the significance of the enhanced structure.

Keywords: Wireless Power Transmission (WPT); Rectangular Spiral; Magnetic Analysis; ANSYS Maxwel; Magnetic Shielding

1. Introduction

The electric vehicle using batteries is a viable solution over traditional transportation because it offers a variety of advantages such as: a clean environment, reduced costs and no congestion charges...etc. However, the restricted capacity for recharging, the high cost, and the short lifespan of the batteries are the main challenges with the aforementioned solution.

Currently, there are two main battery charging methods. The first involves the use of a cable while the second is a current research area and is based on a power Pad supply which is known as wireless power transfer (WPT) [1-2].

 doi:10.20944/preprints202210.0068.v1

The Power Pad is made up of two separate coils, one transmitting and the other receiving. Its operating mechanism is based on the electromagnetic induction theory of energy transmission, in which the magnetic field produced by the first coil on the ground generates a voltage and an electric current between the terminals of the second coil on the vehicle's chassis [3].

Generally, wireless battery charging for EVs can be performed in static or dynamic way. The prime is provided when the car is stationed and the coils are aligned in a parallel position. The second one is produced when the vehicle is moving along the road of the charging coils.

Despite the fact that wireless dynamic charging was more frequently used in a variety of industrial and biomedical fields [4-9] and does not require human presence, there are still some drawbacks to be mentioned. For instance, the coupling decreases, the charging time increases, and the human is not covered from the risks of the magnetic field if there is a considerable distance between the two charging coils.

Consequently, this subject has extremely attracted the attention of researchers and the university of Auckland researchers have made the most significant contributions.

Many magnetic couplers have been proposed to improve the coupling between the charging coils and the efficiency of the Power Pad. However, several studies' percentage efficiencies, particularly for inductive power transfer (IPT), remain below 90% [10-14]. Additionally, the misalignment problem when the vehicle is moving also affected the charging process. Efficiency is reduced when there is a significant misalignment between the two coils. According to [15-17], the authors are mentioned that the coupling coefficient is decreased from 1.6 to 0.2 with a 20% misalignment unlike in the opposite case.

In addition, various solutions are examined and tested to improve the efficiency of these chargers as they can cause some problems, especially when operating at high frequencies. Which can cause some electromagnetic interference. EMF leakage occurs when a proportion of the EMF is emitted around the WPT system during power transfer from the secondary to the primary coil. Electromagnetic loss has an effect on more than just equipment and parts adjacent to the WPT system. It also endangers human health and safety by producing current and heat within the human body, which may irritate muscles and nerve cells and tissues [18-21]. In addition, as stated in [22], the issue of charging speed necessitates a rise in the capacity of EV-WPT systems, which causes higher EMF leakage, as well as the necessity to certify that WPT systems comply with global security criteria [23][24]. The assessment of WPT system exposure in recharge mode and with relation to the influence of body matter have both been the subject of numerous studies [25–27]. The influence of human attitude and related attitudes toward WPT data has been the main focus of the most recent reference. Specifically, the magnetic field produced by a fixed 85 kHz medium frequency (IF) WPT system that is used to charge the FIAT 500 compact car battery [27].

Preprints (www.preprints.org) | NOT PEER-REVIEWED | Posted: 6 October 2022 doi:10.20944/preprints202210.0068.v1

Currently, several investigations on electromagnetic shielding techniques to reduce the emission of electromagnetic fields from WPT systems have currently been conducted in the past few years. Magnetic coupler shielding is generally constructed in one of two configurations: single or double ferrite in the first, but ferrite and an aluminum plate in the second [28–31].

Likewise, the self- and mutual inductance parameters, which make up the coils and offer qualities like the coupling coefficient, are important factors in the magnetic analysis of the coil structures that make up the power pad. However, novel spiral rectangular coupling and other geometries have been integrated into the transformer design to enhance power transfer efficiency, rendering parameter calculations more complex. Luckily, the use of finite element analysis may be able to overcome these limitations.

For many applications involving electromechanical systems, Ansys Maxwell solves static, frequency, and time-varying electric or EM fields and provides specific design interfaces. Especially in the fields of static and time-varying magnetic and electrical analysis by checking the output data with the help of mathematical expression. Also, the coupling coefficient and mutual induction that can be calculated by the electric vehicle during the wireless charging process are also calculated [32].

In this paper, the design of the power pad based on rectangular spiral-shaped for EV charging capacity is investigated according to the distance between two identical rectangular spiral coils with the same number of turns as a function of both the horizontal (X axis) and vertical (Z axis) alignment. The analysis of the magnetic parameters, such as the proper inductance and the mutual separating the two air copper coils of the power supply, as well as the magnetic field or the 3D inductance distribution, is first provided. However, the obtained coupling coefficient is not satisfied and the leakage flux is important. Then, in order to reduce leakage flux, enhance coupling coefficient, and develop a better power system during dynamic charging, the single shielding based on the addition of ferrite and double shielding based on the addition of aluminum processes are employed. Also, the proper and mutual induction parameters separating the transmitter and the receiver as well as a distribution of the magnetic field or induction are analyzed in 3D using ANSYS Maxwell de software in order to predict an adequate shielding structure.

Thus, this article proposes to review the technologies involved in a WPT charger for electric vehicles, in addition to demonstrating a methodology for its design and optimization. In section 2, a description of a WPT charging system for electric vehicles is provided. In section 3, a 3D representation of spiral coils is given. In section 4 and 5 the results acquired during the development of the power system are discussed. Finally, the conclusion is then delivered.

2. Description of WPT system

The system consists of two coils, one transmitting and the other receiving, which will serve as the transformer's primary and secondary windings (Figure 1). The transmitting coil is supplied by an inverter. The DC voltage of the input inverter is provided by a rec-

Preprints (www.preprints.org) | NOT PEER-REVIEWED | Posted: 6 October 2022 doi:10.20944/preprints202210.0068.v1

tifier connected to the grid. Once an AC current is generated in the reception coil (according to Lenz Faraday's law), a rectifier is used to charge the battery. The phenomenon of resonance is exploited in order to have a better transfer of energy. [2].

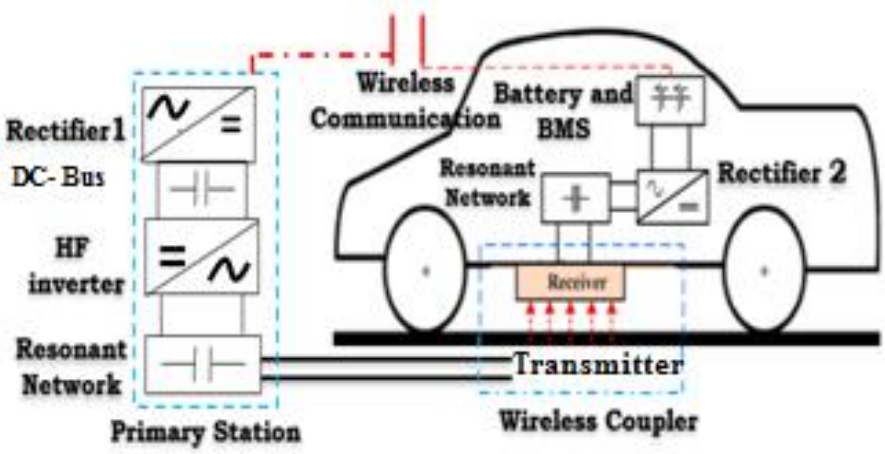

Figure 1. Typical WPT charging system for EVs.

Capacitors are also employed to compensate the enormous positive reactive powers produced by the leakage inductances on both sides of the coils, which enhances the efficiency and performance of power transmission. Thus, they can be placed in either series or parallel to the coupler's windings, providing the four topologies depicted in figure 2.

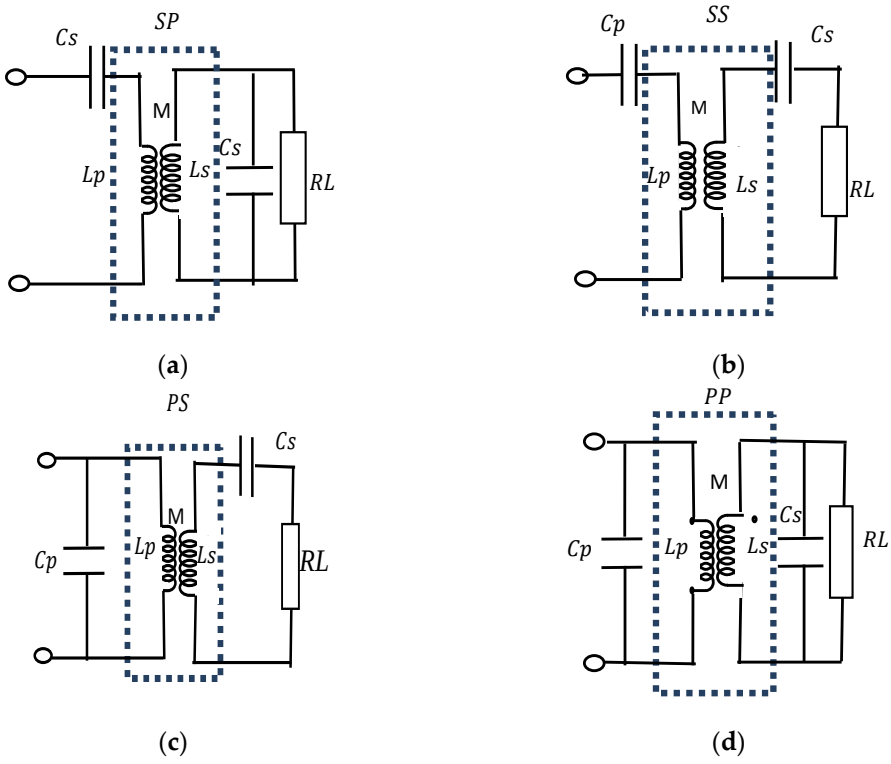

Figure 2. Different topologies of the resonant inductive coupling system: (a) series - parallel, (b) series - series, (c) parallel - series, (d) parallel - parallel.

Preprints (www.preprints.org) | NOT PEER-REVIEWED | Posted: 6 October 2022 doi:10.20944/preprints202210.0068.v1

The WPT system is considered as a single-phase transformer, shown by the equivalent circuit in Figure 3 and the following equations (1) and (2):

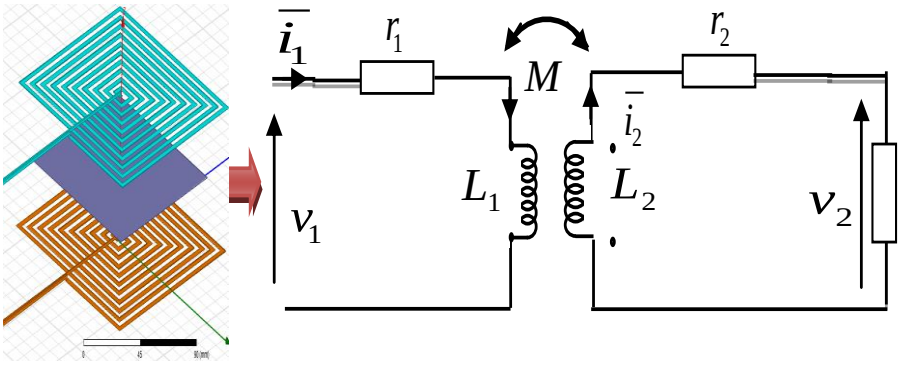

Figure 3. The magnetic circular coupler and its analogous circuit

$$v_1 = L_1 \frac{di_1}{dt} + M \frac{di_2}{dt} + r_1 \cdot i_1 \quad (1)$$

$$v_2 = L_2 \frac{di_2}{dt} + M \frac{di_1}{dt} - r_2 \cdot i_2 \quad (2)$$

These equations can be rewritten using the complex formulation as follows:

$$v_1 = -r_1 \cdot i_1 + jwL_1 i_1 + jwMi_2 \quad (3)$$

$$v_2 = -r_2 \cdot i_2 + jwMi_1 + jwL_2 i_2 \quad (4)$$

Where:

v1, v2: The voltages of the primary and secondary coils

i1, i2: The primary and secondary currents

r1, r2: the resistance of the primary and secondary coils.

L1, L2: the self-inductance of the primary and secondary coils.

M: the mutual inductance between the primary and secondary coils.

3. Description of spiral coils in 3D

The transmitting and receiving coils have been modelled based on 3D presentation using ANSYS Maxwell software. The two coils are formed based on a copper wire with a plan spiral form as shown in Figure 4. The distance between two adjacent wires in each coil, is taken equal to 50 mm. On the other side, a rectangular plate is placed between the transmitter and the receiver coils in the main goal to ensure the capture of the magnetic field.

Copper covers a Size of five hundred millimeter and a width of one millimeter were applied. The simulations would take place fully in the air and would comprise 1000-

Preprints (www.preprints.org) | NOT PEER-REVIEWED | Posted: 6 October 2022 doi:10.20944/preprints202210.0068.v1

square- millimeter areas. Figure 4 depicts design of the rectangular spiral coils without ferrite coil.

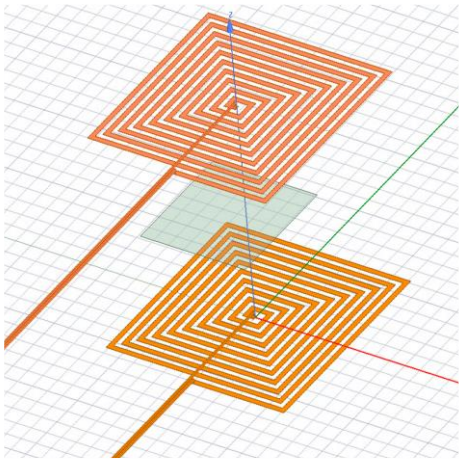

Figure 5. Design of the rectangular spiral coils without ferrite

Table 1 includes information about the coil's properties. Then, tables 2 and 3, respectively, provide information on the characteristics of the rectangular plate and the air region.

Table 1. The coil's properties.

Name	Transmitter Coil	Receiver Coil
Number of Turn	10	10
Width of the spiral coil	3 mm	3 mm
Thickness of the spiral coil	0,0762 mm	0,0762 mm
Distance between turns	6mm	6mm

Table 2. Rectangular plate properties

Command	Coordinate system	Position	Axis	Y size	Z size
Rectangle	global	50,0.70	Z	-70mm	-70mm

Table 3. The Air Region Properties

Name	Value	Unit	Evaluated Value
Command	Created Box		
Coordinate system	Global		
Position	-500, -500 ,-500	mm	-500mm, -500mm, -500mm
Xsize	1000	mm	1000mm
Ysize	1000	mm	1000mm
Wsize	1000	mm	1000mm

4. Simulation Results

Preprints (www.preprints.org) | NOT PEER-REVIEWED | Posted: 6 October 2022 doi:10.20944/preprints202210.0068.v1

As mentioned in reference [9], the authors limited their study for vertical misalignment. In order to carry out a thorough investigation and minimize the exploitation, the two cases of vertical and horizontal misalignment are examined in this study. The ANSYS Maxwell tool is used to perform a three-dimensional simulation and analysis of a spiral rectangular coil transformer. As a preliminary step, the WPT model which has considered previously is examined without ferrite in order to provide the influence of this one on the quality and the quantity of transmitted energy as shown in figure 6.

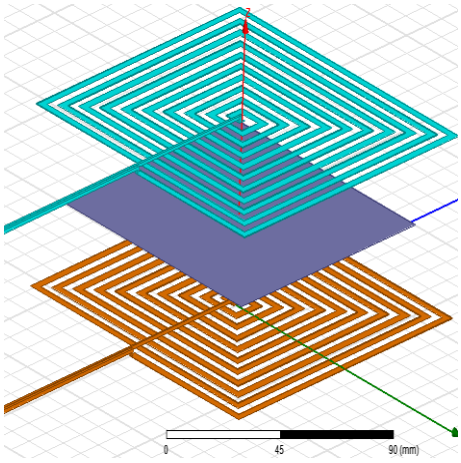

Figure 5. Design of the rectangular spiral coils without ferrite

4.1. Vertical Misalignment

The calculation of the proper and mutual inductances is obtained with the variation of the vertical distances (d) separating the two coils of the model. Figure 6 illustrates the relationship between mutual inductance and distance, showing that the mutual inductance is inversely proportional to the distance between the two coils, representing the amount of energy transmitted. As a result, as the distance between the coils is increased, less energy has been sent to the receiver.

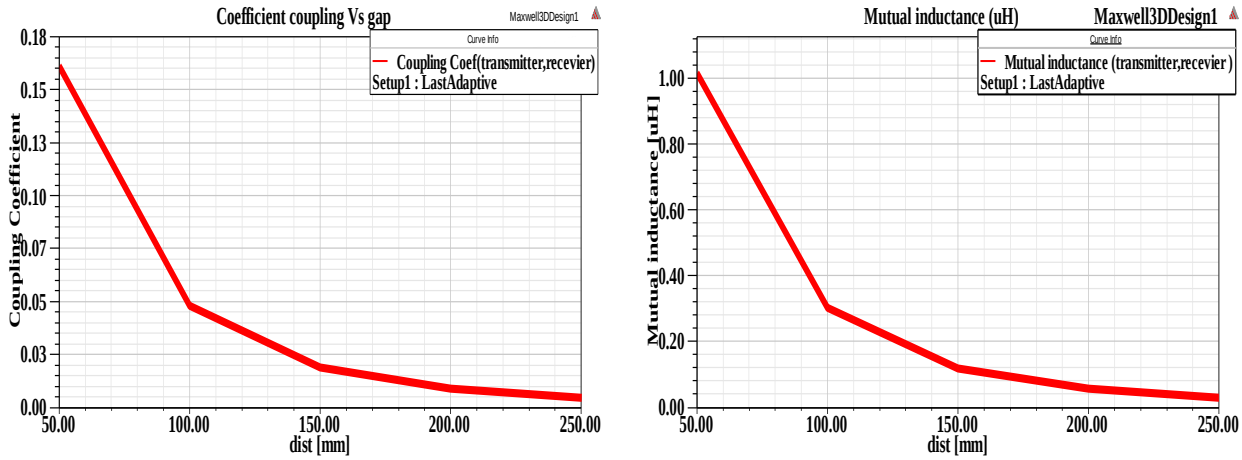

(**a**) (**b**)

Figure 6. (**a**) Coupling coefficient; (**b**) Mutual inductance, under variation of vertical misalignment d=50mm up to 250mm.

Preprints (www.preprints.org) | NOT PEER-REVIEWED | Posted: 6 October 2022 doi:10.20944/preprints202210.0068.v1

The magnetic permeability of the medium in the study model without ferrite (in air) is μr=1. From figures 7 and 8, it is clearly noticeable that the self-inductances of the transmitting and receiving coils are fairly constant despite the variation in vertical distance. Then, the coupling coefficient $K = \frac{M}{\sqrt{L_1 L_2}}$ is varied linearly according to the mutual inductance because L_1 of the transmitter and L_2 of the receiver are almost fixed equal to 6.3μH.

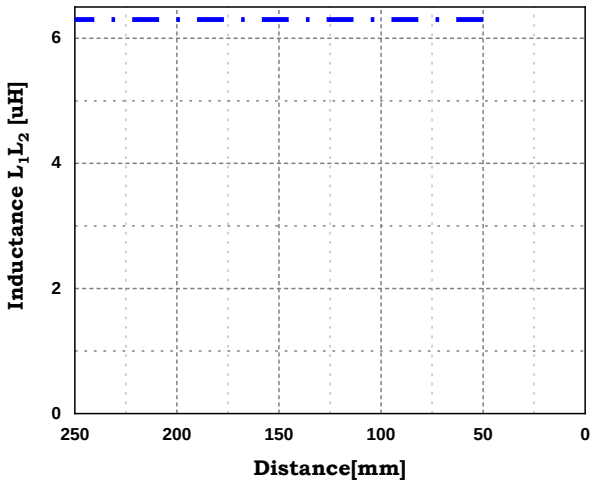

Figure 7. Self-inductances of the rectangular spiral coils without ferrite

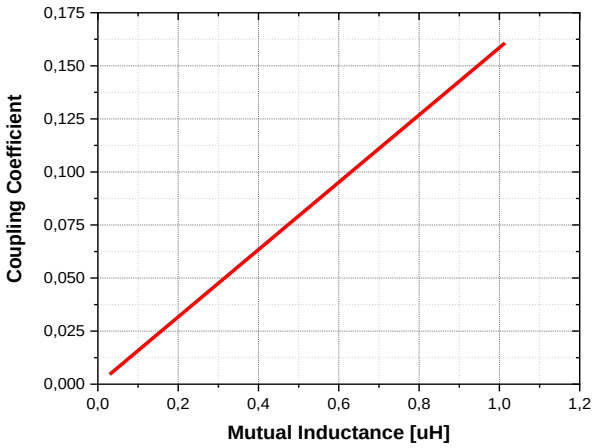

Figure 8. Values the coupling coefficient according to Mutual inductance

In the absence of a saturation phenomenon, designers can apply the linear hypothesis (B=μ.H) to the magnetic induction at any point in the coil's environment (as well as the flux). Under these conditions, the magnetic induction (as well as the flux) is proportional to the current passing through it. The inductance of the winding is constant because the magnetic circuit cannot be deformed as can be seen in figure 9.

Preprints (www.preprints.org) | NOT PEER-REVIEWED | Posted: 6 October 2022 doi:10.20944/preprints202210.0068.v1

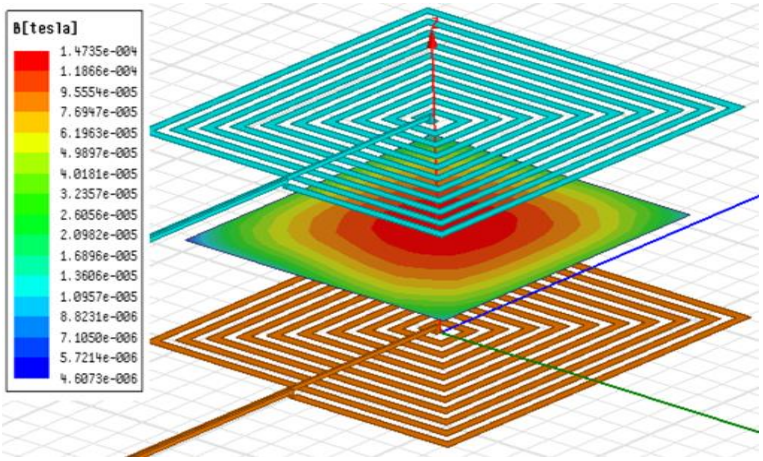

Figure 9. Values the coupling coefficient according to Mutual inductance

The self-inductance can be calculated using analytical formulas. The fundamental dimensional variables of a spiral are N, w, s, dxi and dxo as depicted in figure 10.

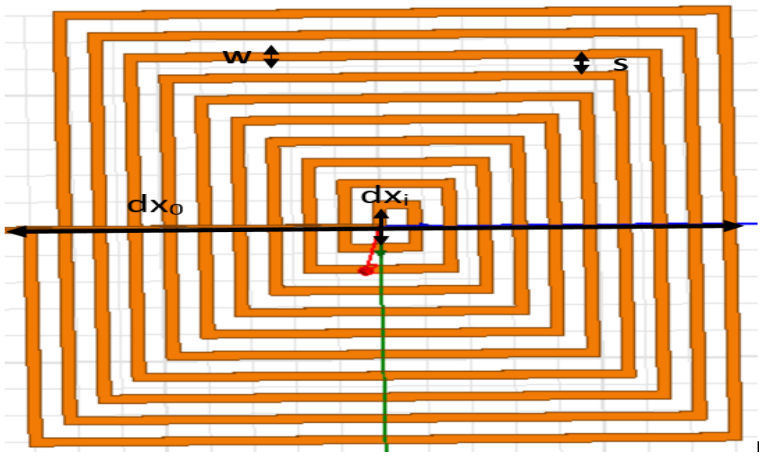

Figure 10. Schematic of the rectengular coil

Where,

N: is the number of turns,

w: is the cross-sectional width,

s: is the spacing between successive turns,

dxi and dxo: are the spiral inner side length and spiral outer side length respectively.

The outer side length dxo is derived from the other geometrical parameters.

$$dx_0 = dx_i + 2\times[N\times w+(N-1)\times s] \quad (6)$$

For a planar spiral square coil, the self-inductance can be calculated as follows [33]:

$$L = 2.34\times\mu_0\times\frac{N^2\times d_{avg}}{1+2,75\times\phi} \quad (7)$$

Where

Preprints (www.preprints.org) | NOT PEER-REVIEWED | Posted: 6 October 2022 doi:10.20944/preprints202210.0068.v1

$$d_{avg} = \frac{dx_0 + dx_i}{2} \tag{8}$$

$$\phi = \frac{dx_0 - dx_i}{dx_0 + dx_i} \tag{9}$$

Based on equation (7), the value of self-inductance of the two coils L1 and L2, is 5µH.

The estimated and simulated self-inductance are presented in table 4.

Table 4. The estimated and simulated self-inductance

Inductances	Simulated value	Calculated value
Inductance L1 L2 (µH)	6,3	5

Magnetic permeability is simply the material's ability to form an internal magnetic field within itself under the influence of an external magnetic field. The higher a material's magnetic permeability, the more effectively is likely to channel magnetic field lines. Figures 11 and 12 show that the magnetic permeability is low in the case of air or vacuum, which results in the non-canalization of the magnetic vector potential field lines, which requires an adequate shielding.

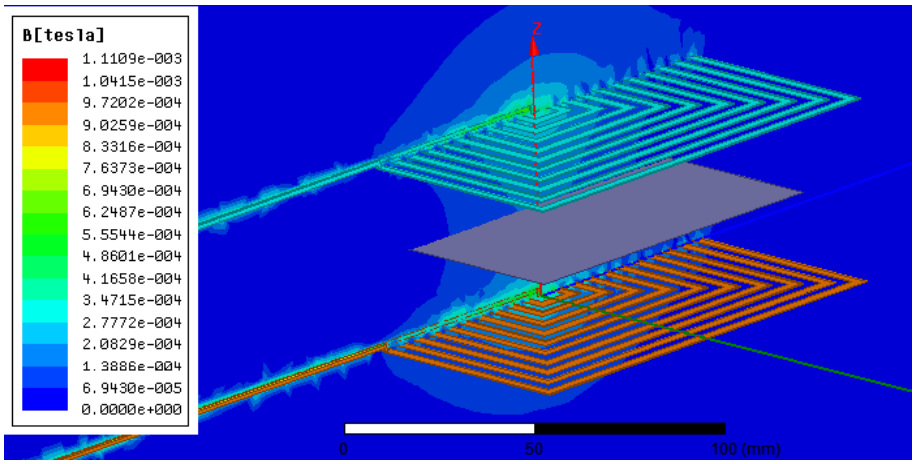

Figure 11. Magnitude of the magnetic field with d=50mm

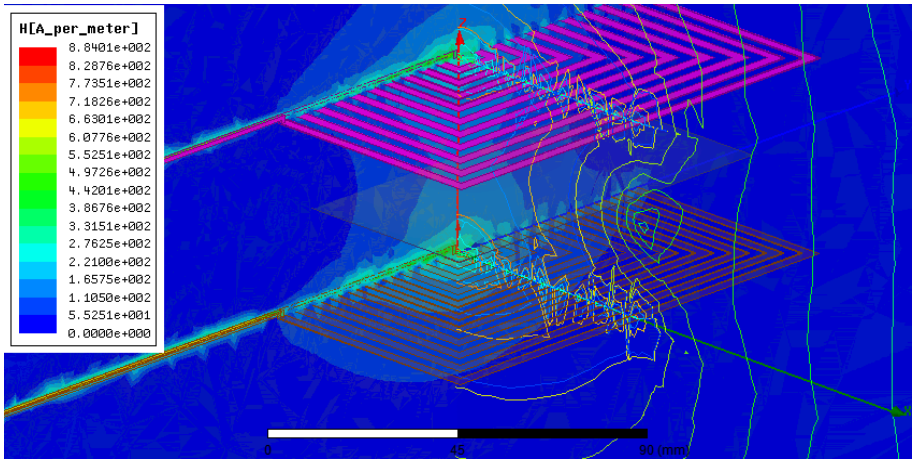

Figure 12. Magnetic field with the field lines separated by 50mm along the ZY axis Plane

4.2. Horizontal misalignment

Preprints (www.preprints.org) | NOT PEER-REVIEWED | Posted: 6 October 2022 doi:10.20944/preprints202210.0068.v1

This section examines the relationship between the coupling coefficient and the horizontal separation distances that range from -40 mm to 40 mm with a step of 10 mm. As well as the relationship between the mutual inductance and the same distances as shown in figure 13.

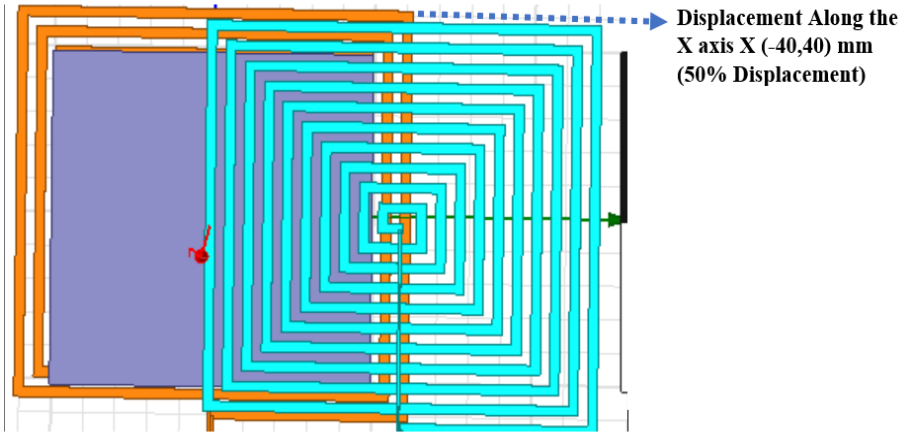

Figure 13. Displacement with misalignment along the X axis

The obtained results demonstrate that tests with horizontal alignment produced parabolic-shaped changes in the coupling coefficient and mutual induction. Both the mutual inductance and the coupling coefficient are decreased as the misalignment is increased. When the misalignment is zero and the two coils are in phase (X=0 mm), the coupling coefficient and mutual inductance also achieve their maximum values. As results, the magnetic coefficients are more effective when the two coils are closely together, as shown in Tables 5 and 6 and figure 14.

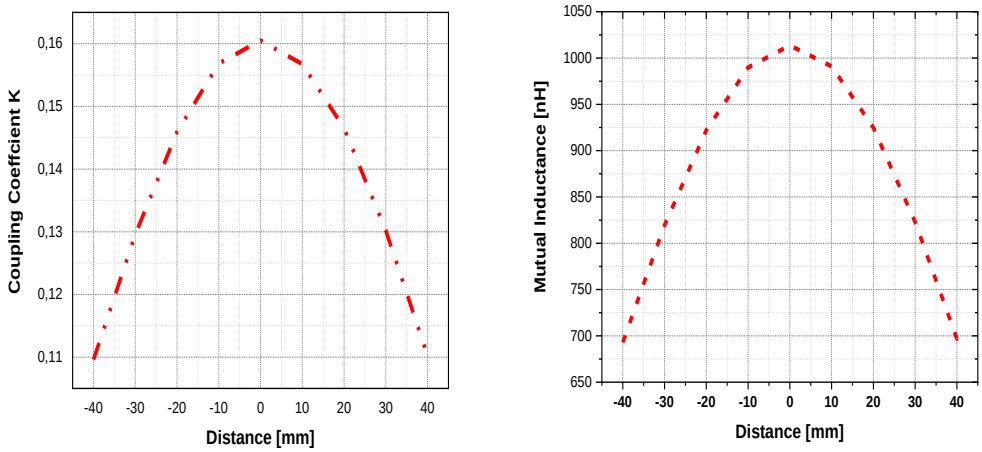

(**a**) (**b**)

Figure 14. Coupling coefficient (a)and Mutual inductance (b) variation of Horizontal misalignment d= - 40mm up to 40mm.

Table 5. Inductor Values obtained from horizontal separation

Preprints (www.preprints.org) | NOT PEER-REVIEWED | Posted: 6 October 2022 doi:10.20944/preprints202210.0068.v1

	Z space [mm]	Mutual inductance [nH]
1	-40	692.976
2	-30	819.490
3	-20	922.116
4	-10	989.814
5	0	1013.691
6	10	991.027
7	20	924.681
8	30	822.780
9	40	696.879

Table 6. Coupling Coefficient Values obtained from horizontal separation

	Z space [mm]	Coupling Coefficient
1	-40	0.109618
2	-30	0.129554
3	-20	0.145936
4	-10	0.156849
5	0	0.160521
6	10	0.156756
7	20	0.146528
8	30	0.130157
9	40	0.110225

5. Design of a Magnetic Coupler Shielding Structure

The magnetic coupler leads to the increase of the magnetic field lines in the active region and the decrease of the magnetic field lines in the inactive region in the energy transfer zone. The two available shielding modes are shown in figure 15.

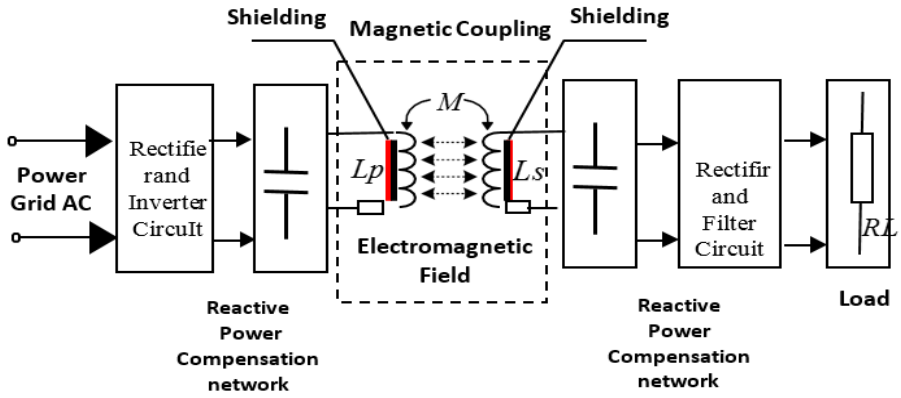

Figure 15. The inductively coupled (WPT) system [18]

5.1 Model With Single Shield In Ferrite Core

Typically, the design of a magnetic coupler should be considered after determining the necessary mutual inductance. According to the literature, the ferrite core can enhance magnetic shielding and mutual inductance for a proper design of the magnetic coupler, particularly when there is a significant air gap as depicted in figure 16. In this first part of

Preprints (www.preprints.org) | NOT PEER-REVIEWED | Posted: 6 October 2022 doi:10.20944/preprints202210.0068.v1

study, a magnetic coupler with and without ferrite cores is simulated using Ansoft Maxwell.

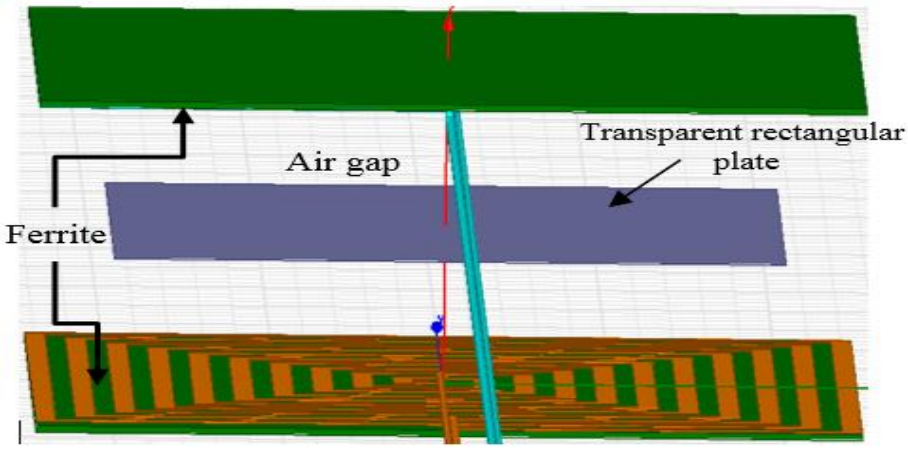

Figure 16. Magnetic coupler with a single shield

According to figures 17 and 18, the mutual inductance is reduced when the air gap between the two coils is increased which provides information on the amount of energy transmitted, i.e., a lower transferred energy results from a greater distance between the two coils.

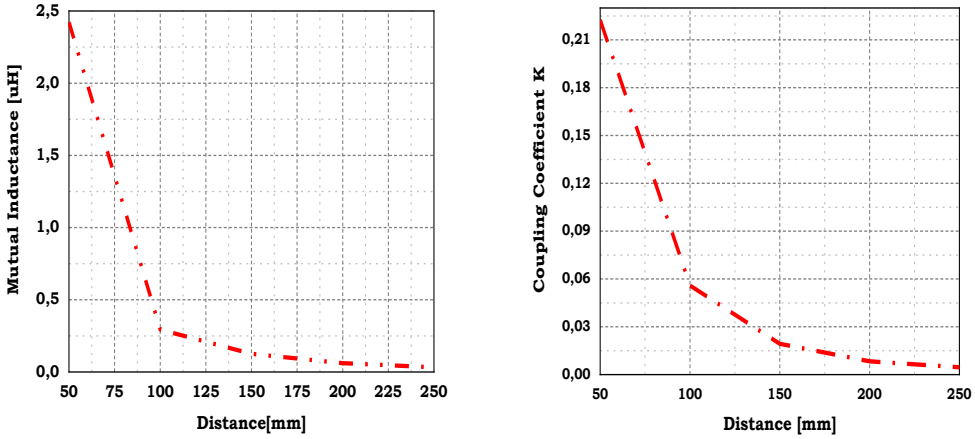

(**a**) (**b**)

Figure 17. Mutual inductance (a) and coupling coefficient (b) with ferrite with variation of d =50mm up to 250mm.

Preprints (www.preprints.org) | NOT PEER-REVIEWED | Posted: 6 October 2022 doi:10.20944/preprints202210.0068.v1

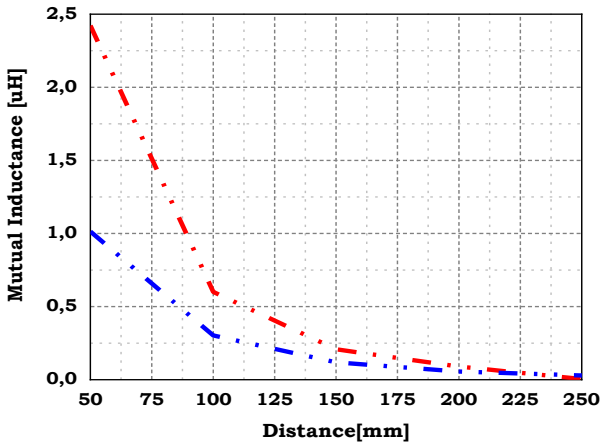

Figure 18. Mutual inductance with and without ferrite of variation the Distance

Figures 19 and 20 show that the values of the self-inductances have increased considerably which is due to the addition of ferrite that has a high magnetic permeability μr≈1000. Nevertheless, the variation of the self-inductances is important for the small air gap because the ferrite strongly contributes to the distribution of the magnetic field.

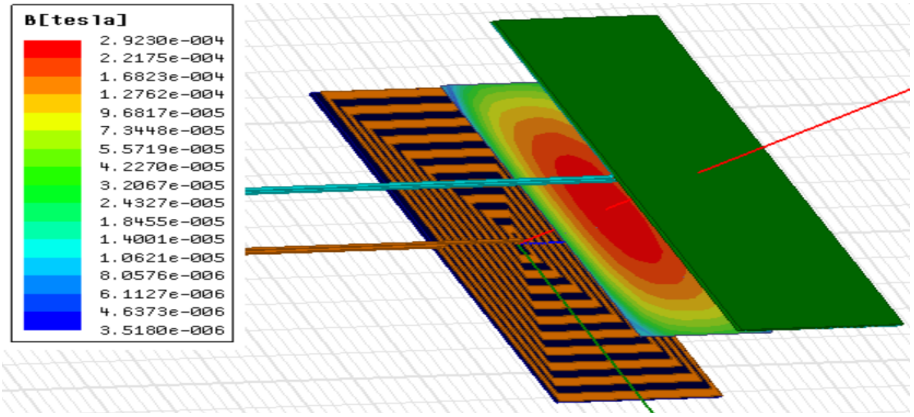

Figure 19. Magnitude of the magnetic induction with ferrite d=50mm

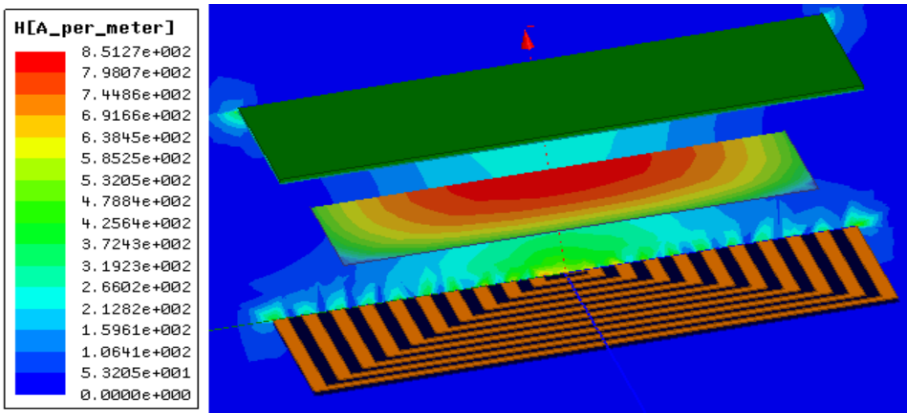

Figure 20. Magnetic field Along the ZY axis With the field lines with ferrite d=50mm

Preprints (www.preprints.org) | NOT PEER-REVIEWED | Posted: 6 October 2022 doi:10.20944/preprints202210.0068.v1

Consequently, when the mutual inductance is increased, flux and EMF also is increased. The distribution of magnetic field lines is much more channeled and it is propagated from the transmitting coil to the outside and close on the magnetic circuit (ferrite), indicating that the ferrite material provides shielding.

5.2.Model with double shield in ferrite core and aluminum

The single shielding of the WPT model discussed above is improved in this second section by using a double shielding where it is made by adding aluminum to the ferrite. The simulations are conducted using an eddy current solution with a frequency of 85 kHz and a constant current (1A) of the transmission coil. The appropriate and mutual inductances are determined by varying the vertical distance (d) between the model's two coils, as shown in figure 21.

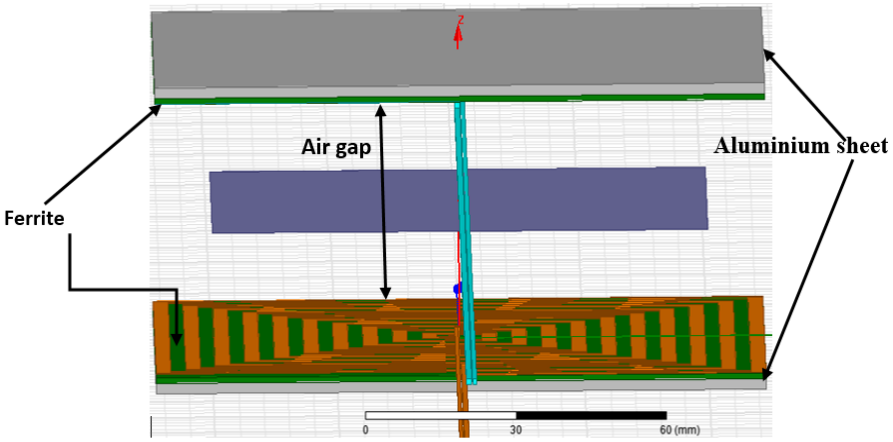

Figure 21. Magnetic coupler with a double shield

As shown in figure 22, the values of the mutual inductance and coupling coefficient obtained using a double shield are similar to those obtained using a single shield.

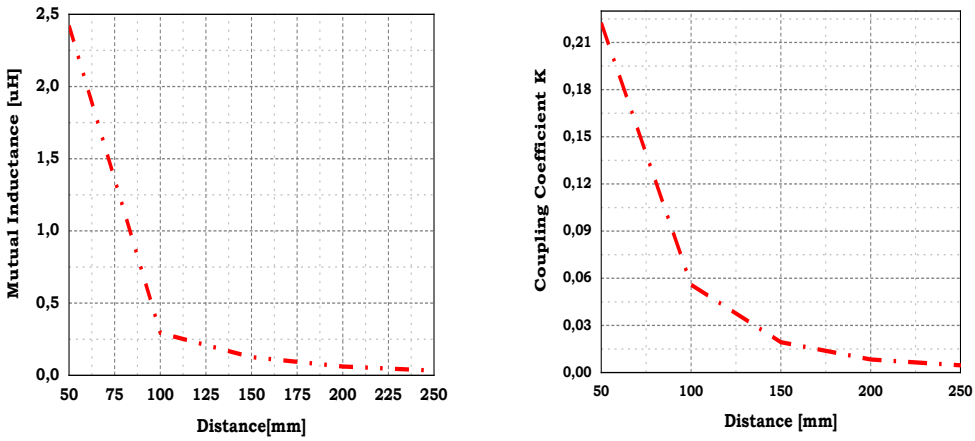

(**a**) (**b**)

Figure 22. (a) Mutual inductance ; (b) coupling coefficient , with ferrite and a variation of d =50mm up to 250mm.

Preprints (www.preprints.org) | NOT PEER-REVIEWED | Posted: 6 October 2022 doi:10.20944/preprints202210.0068.v1

Although the magnetic field generated above, the vehicle's receiving coil is considerably reduced by the ferromagnetic core, once the magnetic flux enters the chassis, it can cause eddy current losses and interfere with the electrical components. Therefore, magnetic shielding is considered. As shown in figures 23, 24, 25 and 26, the magnetic field above the receiver is decreased owing to the tailored aluminum foil as well as eddy currents are concentrated above the coils of the magnetic coupler.

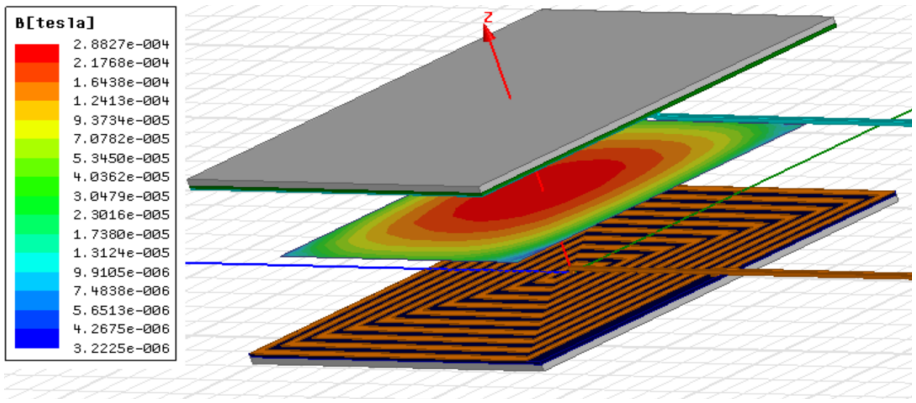

Figure 23. Magnitude of the magnetic induction with ferrite plus Aluminum d=50mm

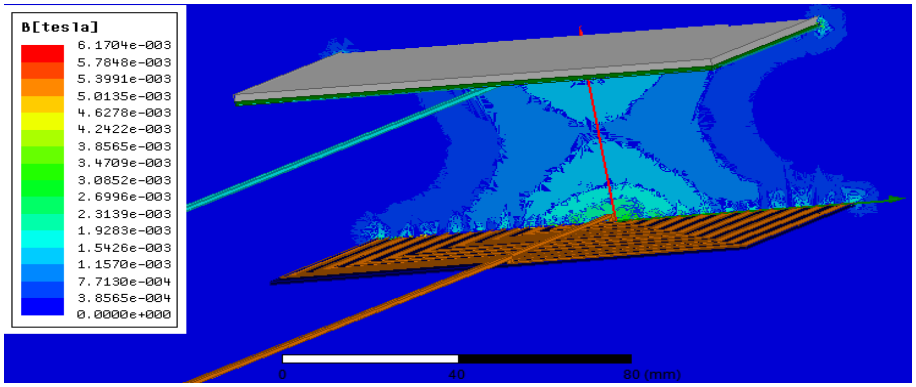

Figure 24. Magnetic field Along the ZY axis With the field lines with ferrite d=50mm

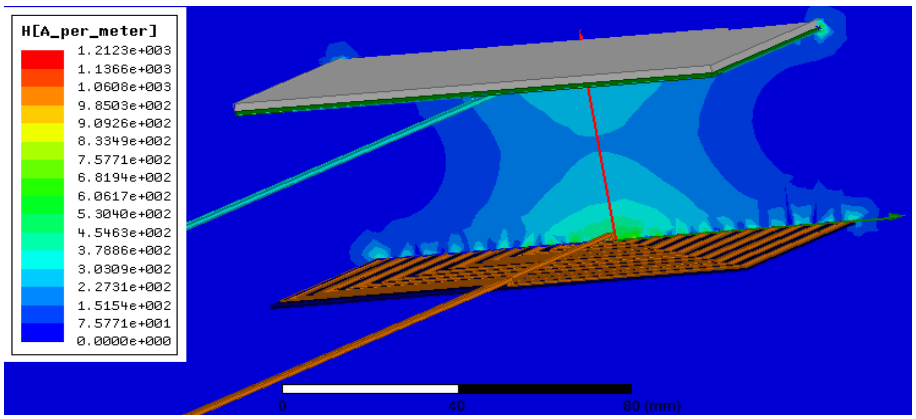

Figure 25. (a) Magnetic field Along the ZY axis With the field lines with ferrite and Aluminum d=50mm

Preprints (www.preprints.org) | NOT PEER-REVIEWED | Posted: 6 October 2022 doi:10.20944/preprints202210.0068.v1

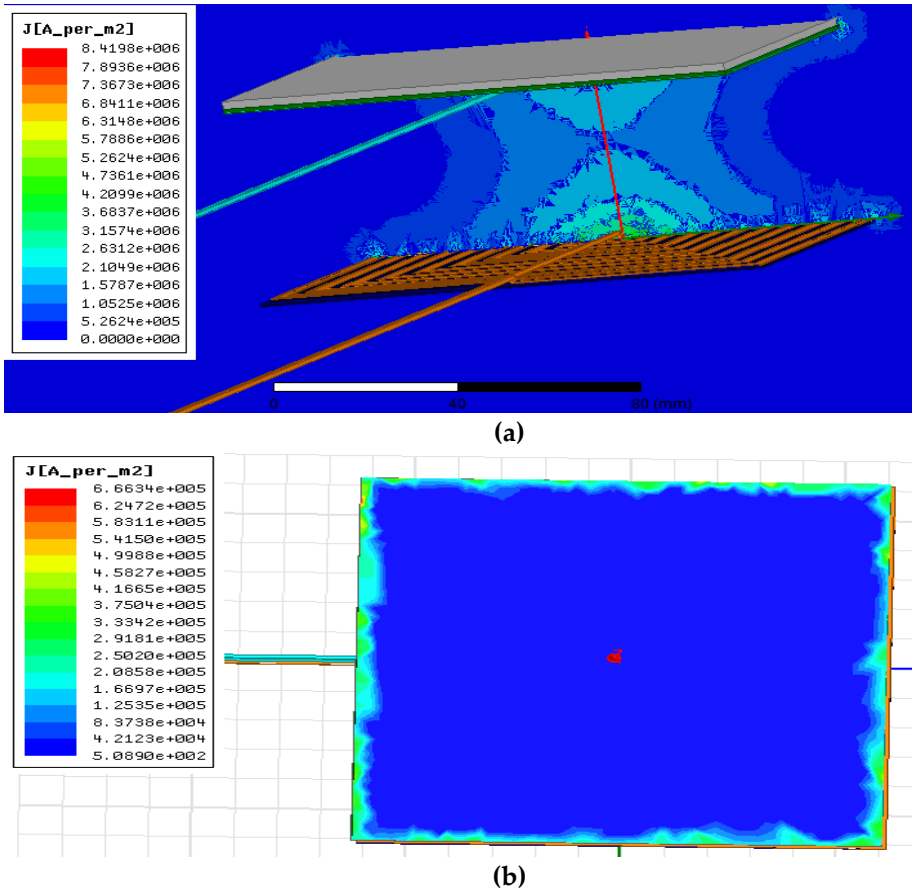

Figure 26. (a) Simulation model and eddy current density and (b) Magnetic field with/without Aluminum sheet (Yellow: Litz coil, green: ferrite cores, and dark grey : Aluminum sheet).

6. Conclusions

In this article, three cases of magnetic coupling between two identical rectangular spiral coils with the same number of turns depending on both the horizontal (X axis) and vertical (Z axis) alignment were studied in order to optimize the power supply for electric vehicle (EV) charging. The obtained results show that the primary and secondary self-inductances are constant and independent of the distance between the two coils, in the same time the magnetic coupling is enhanced by the higher mutual achieved across a shorter distance where the estimated (5 μH) and simulated (6.3 μH) self-inductances values are very close. Furthermore, the obtained results from the distribution of the magnetic field have shown that the line of the field is outside the area between the two coils which requires an effective shielding. Consequently, after the insertion of the ferrite which is a high permeability magnetic material, the coupling coefficient is improved. However, the first shielding remains insufficient. On the other side, the insertion of aluminum has shown more effective and sufficient shielding without the coupling coefficient changing. As a perspective to the work presented in this paper, the obtained results can be enhanced and experimentally validated by using other materials and shapes.

Author Contributions: Conceptualization, N.B. and L.K.; methodology, N.B., L.K, I.B. and K.A; software, N.B, L.K. and I.B.; validation, N.B., L.K, I.B. and K.A; formal analysis, N.B., L.K, I.B. and K.A;

investigation, N.B., L.K, I.B., K.A, B.A., R.K., M.A. X.X.; resources, N.B., L.K, I.B. and K.A; data curation, N.B., L.K, and I.B.; writing—original draft preparation, N.B., L.K, I.B. and K.A; writing—review and editing, N.B., L.K, I.B.,K.A, R.K. and M.A.; visualization, N.B., L.K, I.B. and K.A; supervision, N.B., L.K, I.B.,K.A, R.K. and M.A; project administration, N.B., L.K, I.B.,K.A, R.K. and M.A; funding acquisition, R.K. and M.A. All authors have read and agreed to the published version of the manuscript

Funding: This project was financially supported by the Directorate General for Scientific Research and Technological Development of the Algerian Ministry of Higher Education and Scientific Research in Algeria, and the Laboratory of Applied automation and Industrial Diagnostics of Djelfa University, Algeria.

Institutional Review Board Statement: Not applicable.

Informed Consent Statement: Not applicable.
Data Availability Statement: Not applicable.

Acknowledgments: Not applicable.

Conflicts of Interest: The authors declare no conflict of interest.

References

1. Lassioui, A.; Fadil, H.E.; Belhaj, F.Z.; Rachid, A. Battery Charger for Electric Vehicles Based ICPT and CPT-A State of the Art. In Proceedings of the 2018 Renewable Energies, Power Systems Green Inclusive Economy (REPS-GIE), Casablanca, Morocco,23–24 April 2018; pp. 1–6.
2. Kim, J.; Kim, J.; Kong, S.; Kim, H.; Suh, I.-S.; Suh, N.P.; Cho, D.-H.; Kim, J.; Ahn, S. Coil Design and Shielding Methods for a Magnetic Resonant Wireless Power Transfer System. Proc. IEEE 2013, 101, 1332–1342, doi:10.1109/JPROC.2013.2247551.
3. Daniel Ongayo and Moin Hanif, Member, IEEE"Comparison Of Circular And Rectangular Coil Transformer" Conference Paper · November 2015DOI: 10.1109/COBEP.2015.7420222
4. Cui, H.; Zhong, W.; Li, H.; He, F.; Chen, M.; Xu, D. A study on the shielding for wireless charging systems of electric vehicles. In Proceedings of the 2018 IEEE Applied Power Electronics Conference and Exposition (APEC), San Antonio, TX, USA, 4–8 March 2018; pp. 1336–1343.
5. Campi, T.; Cruciani, S.; Feliziani, M.; Maradei, F. Magnetic field generated by a 22 kW–85 kHz wireless power transfer system for an EV. In Proceedings of the 2017 AEIT International Annual Conference, Cagliari, Italy, 20–22 September 2017.
6. Wang, Q.; Li, W.; Kang, J.; Wang, Y. Electromagnetic safety of magnetic resonant wireless charging system in electric vehicles. In Proceedings of the 2017 IEEE PELS Workshop on Emerging Technologies: Wireless Power Transfer (WoW), Chongqing, China, 20–22 May 2017.
7. Wang, Q.; Li, W.; Kang, J.; Wang, Y. Magnetic Field Distribution in a WPT System for Electric Vehicle Charging. In Proceedings of the Progress in Electromagnetic Research Symposium (PIERS), Shanghai, China, 8 August–11 September 2016; p. 5165.
8. Sibakoti, M.J.; Hambleton, J. Wireless Power Transmission Using Magnetic Resonance; Cornell College PHY312: Mount Vernon, IA, USA, 2011.
9. El-Shahat, A.; Ayisire, E. Novel Electrical Modeling, Designand Comparative Control Techniques for Wireless Electric Vehicle Battery Charging. Electronics 2021, 10, 2842. https://doi.org/10.3390/ electronics10222842
10. Kadem, K.; Bensetti, M.; LeBihan, Y.; Labouré, E.; Debbou, M.Optimal Coupler Topology forDynamicWireless Power Transfer forElectric Vehicle. Energies 2021, 14,3983. https://doi.org/10.3390/
11. Ahmed A.S. Mohameda,b,Ahmed A. Shaiera, Hamid Metwallya, Sameh I. Selema A comprehensive overview of inductive pad in electric vehicles,stationaryCharging.https://doi.org/10.1016/j.apenergy.2020.114584
12. Yang YangJinlong Cui and Xin Cui 2Design and Analysis of Magnetic CoilsforOptimizingthe Coupling CoeffcientinanElectricVehicleWireless Power Transfer System,Energies 2020, 13, 4143; https:doi:10.3390/en13164143.
13. Ahmad, A., Alam, M.S., Chabaan, R., and Mohamed, A., "Comparative Analysis of Power Pad for Wireless Charging of ElectricVehicles," SAE Technical Paper 2019-01-0865, 2019, doi:10.4271/2019-01-0865.
14. Benalia N ,Kouider L ,Benlaloui I Improvement of the Magnetic Coupler design for Wireless Inductive Power Transfer.InThe 5th International Conference on Power Electronics and their Applications ICPEA 2022, 29-30 March 2022, Hail, KSA IEEE; 10.1109/ICPEA51060.2022.9791150
15. Budhia, M.; Covic, G.A.; Boys, J.T. Design and Optimization of Circular Magnetic Structures for Lumped Inductive Power Transfer Systems. IEEE Trans. Power Electron. 2011, 26, 3096–3108, doi:10.1109/TPEL.2011.2143730.
16. Budhia, M.; Covic, G.; Boys, J. A New IPT Magnetic Coupler for Electric Vehicle Charging Systems. In Proceedings of the IECON 2010—36th Annual Conference on IEEE Industrial Electronics Society, Glendale, AZ, USA, 7–10 November 2010; pp. 2487–2492.
17. GAO, Y., A. Ginart, K.B. Farley, and Z.T.H. Tse. "Misalignment Effect on Efficiency of Wireless Power Transfer for Electric Vehicles." 2016 IEEE Applied Power Electronics Conference and Exposition (APEC), (2016): 16: 24.
18. De Santis, V.; Giaccone, L.; Freschi, F. Chassis Influence on the Exposure Assessment of a Compact EV during WPT Recharging Operations. Magnetochemistry 2021, 7, 25.

19. De Santis, V.; Giaccone, L.; Freschi, F. Influence of Posture and Coil Position on the Safety of a WPT System While Recharging a Compact EV. Energies 2021, 14, 7248. https:// doi.org/10.3390/en14217248
20. Yuan Li ,Shumei Zhang and Ze ChengDouble-Coil Dynamic Shielding Technology for Wireless Power Transmission in Electric VehiclesEnergies 2021, 14, 5271. https://doi.org/10.3390/en14175271
21. HeqiXu , Chunfang Wang , Dongwei Xia and Yunrui Liu, Design of Magnetic Coupler for Wireless Power Transfer. Energies 2019, 12, 3000; doi:10.3390/en12153000
22. International SAE J2954. Wireless Power Transfer for Light-Duty Plug-In/Electric Vehicles and Alignment Methodology; SAE International:Warrendale PA, USA, 2019.
23. IEEE C95.1-2019. IEEE Standard for Safety Levels with Respect to Human Exposure to Electric, Magnetic, and Electromagnetic Fields, 0 Hz to 300 GHz; IEEE Press: Piscataway, NJ, USA, 2019.
24. ICNIRP. Guidelines for Limiting Exposure to Time-Varying Electric and Magnetic Fields (1 Hz–100 kHz). Health Phys. 2010, 99, 818–836. [CrossRef] [PubMed]
25. Park, S.W.;Wake, K.;Watanabe, S. Incident electric field effect and numerical dosimetry for a wireless power transfer system using magnetically coupled resonances. IEEE Trans. Microw. Theory Tech. 2013, 61, 3461–3469.
26. De Santis, V.; Campi, T.; Cruciani, S.; Laakso, I.; Feliziani, M. Assessment of the Induced Electric Fields in a Carbon-FiberElectrical Vehicle Equipped with aWireless Power Transfer System. Energies 2018, 11, 684.
27. Arduino, A.; Bottauscio, O.; Chiampi, M.; Giaccone, L.; Liorni, I.; Kuster, N.; Zilberti, L.; Zucca, M. Accuracy Assessment of Numerical Dosimetry for the Evaluation of Human Exposure to Electric Vehicle Inductive Charging Systems. IEEE Trans. Electromag. Compat. 2020, 62, 1939–1950.
28. Dolara, A., S. Leva, M. Longo, F. Castelli-Dezza, and M. Mauri. “Coil Design and Magnetic Shielding of a Resonant Wireless Power Transfer System for Electric Vehicle Battery Charging.” 6th International Conference on Renewable Energy and Research and Applications (2017): 143: 151.
29. Cui, H.; Zhong, W.; Li, H.; He, F.; Chen, M.; Xu, D. A study on the shielding for wireless charging systems of electric vehicles. In Proceedings of the 2018 IEEE Applied Power Electronics Conference and Exposition (APEC), San Antonio, TX, USA, 4–8 March 2018; pp. 1336–1343.
30. Kim, J.; Kim, J.; Kong, S.; Kim, H.; Suh, I.-S.; Suh, N.P.; Cho, D.-H.; Kim, J.; Ahn, S. Coil Design and Shielding Methods for a Magnetic Resonant Wireless Power Transfer System. Proc. IEEE 2013, 101, 1332–1342, doi:10.1109/JPROC.2013.2247551.
31. Xu, D.; Zhang, Q.; Li, X. Implantable Magnetic Resonance Wireless Power Transfer System Based on 3D Flexible Coils. Sustainability 2020, 12, 4149.
32. Md Rakib Raihan Razu, Sultan Mahmud, Mohammad Jalal Uddin, Sikder Sunbeam Islam et al. "Wireless Charging of Electric Vehicle While Driving", IEEE Access, 2021
33. Mohan, S. S., del Mar Hershenson, M., Boyd, S. P., & Lee, T. H. (1999). Simple accurate expressions for planar spiral inductances. IEEE Journal of Solid-State Circuits, 34(10), 1419–1424. doi:10.1109/4.792620